Electronic Supplementary Material (ESI) for Nanoscale.

One-step synthesis and XPS investigations of chiral NHC-Au(0)/Au(I) nanoparticles

Adam J. Young,[a] Markus Sauer,[b] Guilherme M. D. M. Rubio,[c] Akiko Sato,[d] Annette Foelske,[b] Christopher J. Serpell,[d] Jia Min Chin*[ac] and Michael R. Reithofer*[c]

a. *Gray Centre for Advanced Materials, School of Mathematics and Physical Sciences, University of Hull, Cottingham Road, Hull, East Riding of Yorkshire, HU6 7RX, UK. E-mail: j.chin@hull.ac.uk*
b. *Vienna University of Technology, Analytical Instrumentation Center, Getreidemarkt 9/BL01A01, A-1060 Wien, Austria*
c. *Institute of Inorganic Chemistry, University of Vienna, Faculty of Chemistry, Währinger Strasse 42, 1090 Vienna, Austria. E-mail: Michael.reithofer@univie.ac.at*
d. *University of Kent, School of Physical Sciences, Ingram Building Canterbury, Kent, CT2 7NH, UK*

Table of Contents

General Considerations

All experiments were performed in air except for the synthesis of **2(L)** and **2(D)** which were performed under a nitrogen atmosphere using Schlenk techniques. *N*-BOC-L-histidine was purchased from GL Biochem (Shanghai) Ltd and used as received. *N*-BOC-D-histidine was purchased from Novabiochem and used as received. Sodium borohydride was purchased from Lancaster chemicals and used as received. Potassium carbonate and methyl iodide were purchased from Fluorochem and used as received. Chloroauric acid and borane tert-butylamine complex was purchased from Alfa Aesar and used as received. Acetonitrile, dichloromethane, *N*,*N*-dimethylformamide, chloroform, toluene, tetrahydrofuran and diethyl ether were purchased from VWR chemicals and used as received. Chloro(dimethyl sulfide) gold was synthesised according to literature procedure.[1] **1L**, **1D**, **2L** and **2D** were synthesised as previously reported.[2]

^{1}H and ^{13}C NMR spectra were recorded on a Jeol JEOL ECZ 400S spectrometer, with TMS δ_H = 0 as the internal standard or residual protic solvent peak [$CDCl_3$, ∂_H = 7.26]. Chemical shifts are given in ppm (δ) and coupling constants (J) are given in Hertz (Hz). Jeol Delta v5.0.4. was used to analyse the NMR spectra. Dynamic light scattering (DLS) size measurements were obtained using a Malvern Zetasizer nano ZS-series, in which each AuNP sample was sonicated before undergoing measurment. Ultraviolet-visible (UV-vis) spectroscopy was carried out using a PerkinElmer spectrophotometer Lambda 25.

The average diameter (D) and the size distribution of the nanoparticles were determined by using ImageJ software and by measuring 100 nanoparticles in arbitrarily chosen areas of the photographs. The size distribution is reported as the standard deviation (σ) which is calculated according to the following formula: $\sigma = \{(D_i - D)^2/ (n - 1)\}^{1/2}$.

Circular dichroism measurements were recorded using a Jasco J-715 spectropolarimeter, with temperature control provided by a NesLab RTE-111 circulating chiller operating at 20 ± 0.05 °C. Spectra were recorded in a 0.2 cm pathlength quartz cell, maintaining consistent cell orientation. Samples were prepared at 1 mg mL^{-1} in dichloromethane (DCM). Spectra were averaged over 20 readings, and subsequently smoothed using a 9-point moving average, followed by subtraction of a similarly smoothed pure solvent baseline.

Electrospray-ionisation MS (ESI-MS) data were acquired using an Agilent 1100 series HPLC coupled with a Bruker HCT Ultra ion trap MS/ MS instrument, operated in the positive mode. Electrospray ion source, capillary voltage 4.0 kV, gas temperature 300 ºC, gas flow 10

L min^{-1}. The samples were diluted in CH_3CN/H_2O/HCOOH (50:49.9:0.1) AND 5µL was introduced into the mass spectrometer.

TEM solid samples were dispersed in dichloromethane or toluene. 5µL drops of all samples were put onto carbon-coated copper grids and allowed to air dry. Images were obtained using Gatan Orius SC600 with a CCD camera systemattached to a Philips CM200 TEM running at 200kV. EDS data were obtained at the same time using an Oxford Instruments INCA Energy EDS system.

XPS analysis of AuNPs. The measurement series was carried out on a SPECS XPS-spectrometer equipped with a monochromatised Al-Kα X-ray source (µFocus 350) and a hemispherical WAL-150 analyser (acceptance angle: 60°).

All samples were mounted onto the sample holder using double-sided carbon tape.
Pass energies of 100 eV and 30 eV and energy resolutions of 1 eV and 100 meV were used for survey and detail spectra respectively (excitation energy: 1486.6 eV, beam energy and spot size: 70 W onto 400 µm, angle: 51° to sample surface normal, base pressure: 9x10-10 mbar, pressure during measurements: 3x10-9 mbar).

Low energy electrons from a broad spot flood gun (SPECS FG 22, e- at 5eV, 25 µA) were used to minimise charging effects during XPS measurements.

Data analysis was performed using CASA XPS software, employing transmission corrections (as per the instrument vendor's specifications), Shirley/Tougaard backgrounds[3, 4] and Scofield sensitivity factors[5]. Charge correction was applied so the adventitious carbon peak (C-C peak) was shifted to approximately 284.8 eV binding energy (BE).
All content values shown are in units of relative atomic percent (at%), where the detection limit in survey measurements usually lies around 0.1-0.5 at%, depending on the element. The accuracy of XPS measurements is around 10-20% of the values shown.

Stability studies of **3'-NP(L)** and **3'-NP(D)** were conducted by dispersing an amount of AuNP in either chloroform, DMF or THF and heated/refluxed at 100 ºC and the UV-Vis spectrum measured at hourly intervals for each sample. A further sample containing the AuNPs dispersed in THF was left at room temperature and the stability of these particles was measured over a longer time period.

Fig. S1. ^{1}H NMR spectrum of **3'-NP(L)**

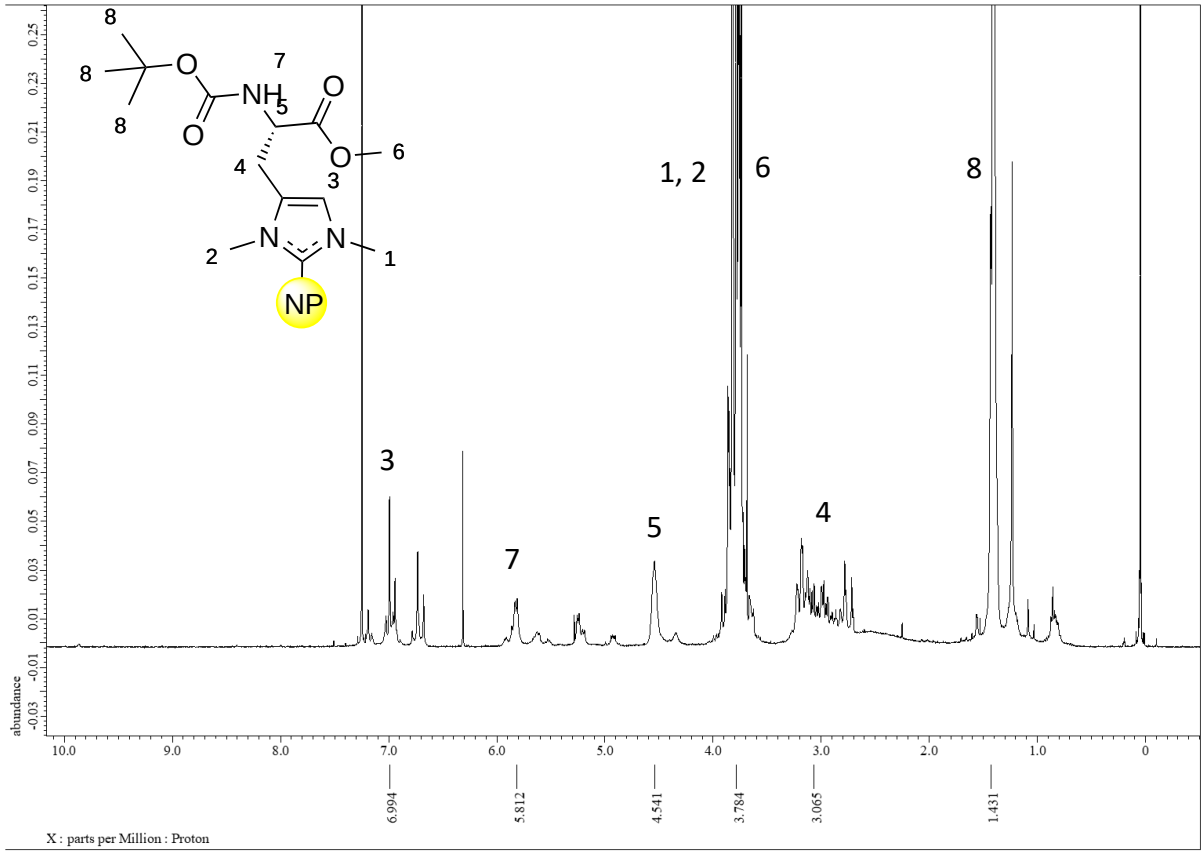

Fig. S2. ^{13}C NMR spectrum of **3'-NP(L)**

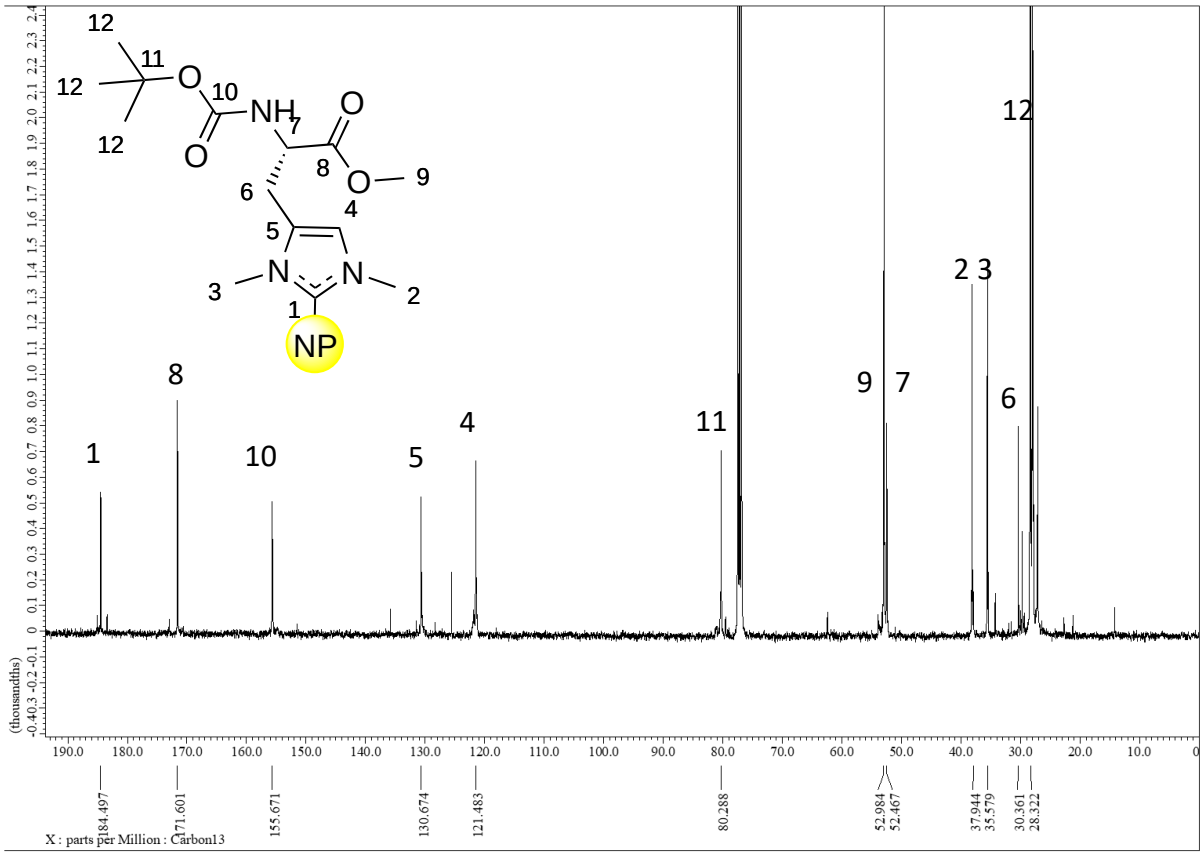

Fig. S3. ^{1}H NMR spectrum of **3'-NP(D)**

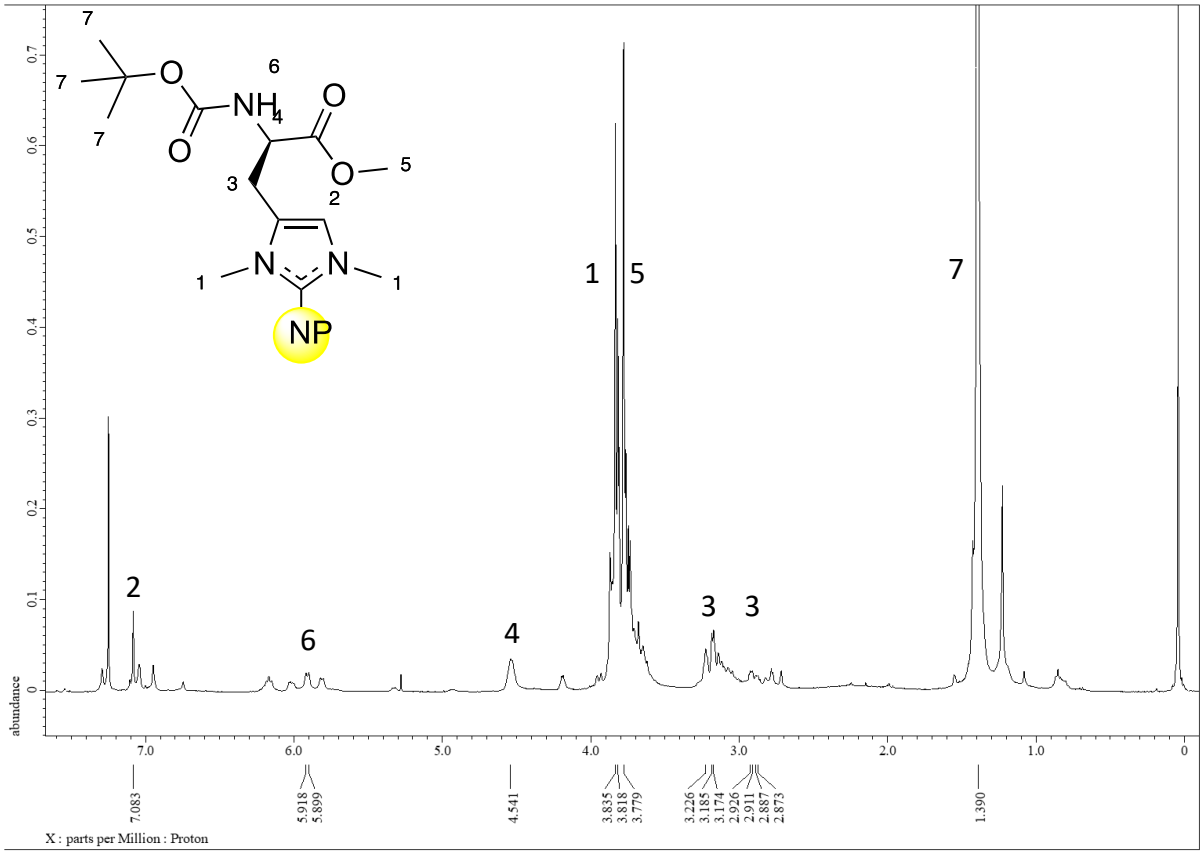

Fig. S4. ^{13}C NMR spectrum of **3'-NP(D)**

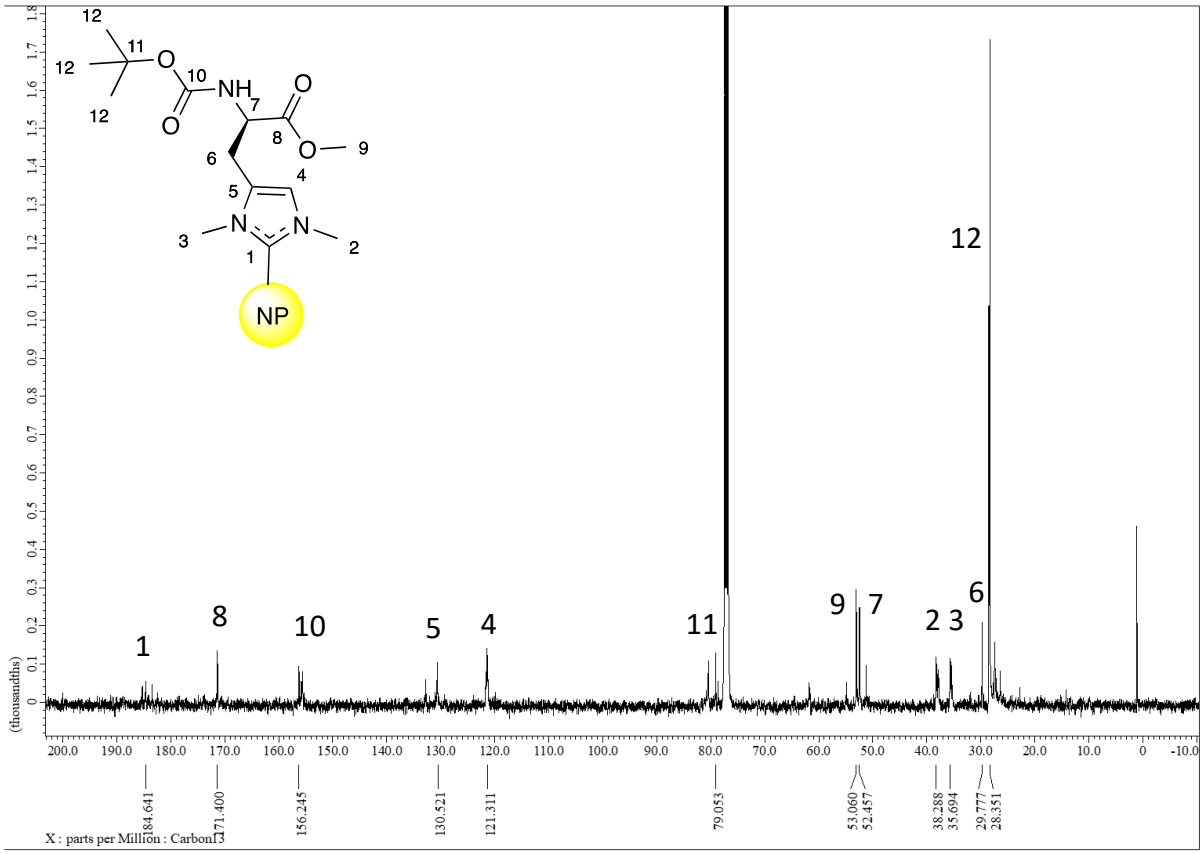

Fig. S5. ^{13}C NMR spectra overlay of **2(L)**, **3'-NP(L)** and a mixture of both **3'-NP(L)+2(L)**

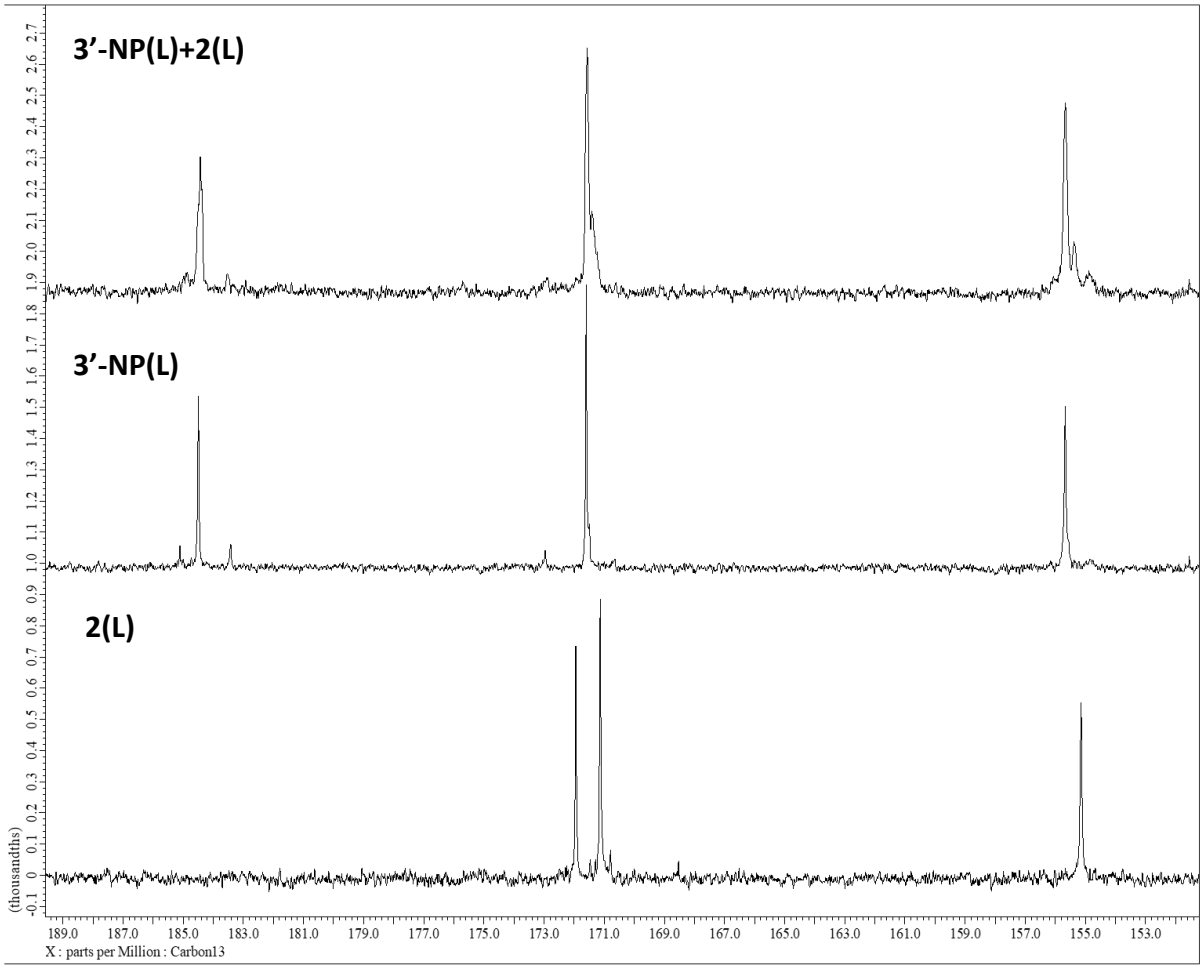

NMR spectra of AuNP/Au-complex mixture indicates the presence of two different species present in the NMR spectrum. The overlapping broad peak seen at ~171 ppm is indicative of the presence of the Au(I) starting material as well as the carbonyl carbons present in both species. Furthermore, the presence of a two peaks at ~155 ppm clearly shows two different species present and only one peak is is observed at ~184 ppm demonstrating that this peak only originates from the AuNPs themselves and not any remaining Au(I) complex.

Fig. S6. Photographs of **3'-NP(L)** synthesis: a) **2(L)** in DCM before addition of $NaBH_4$ aqueous solution, b) **3'-NP(L)** after reaction being worked up and being re-dispersed in DCM.

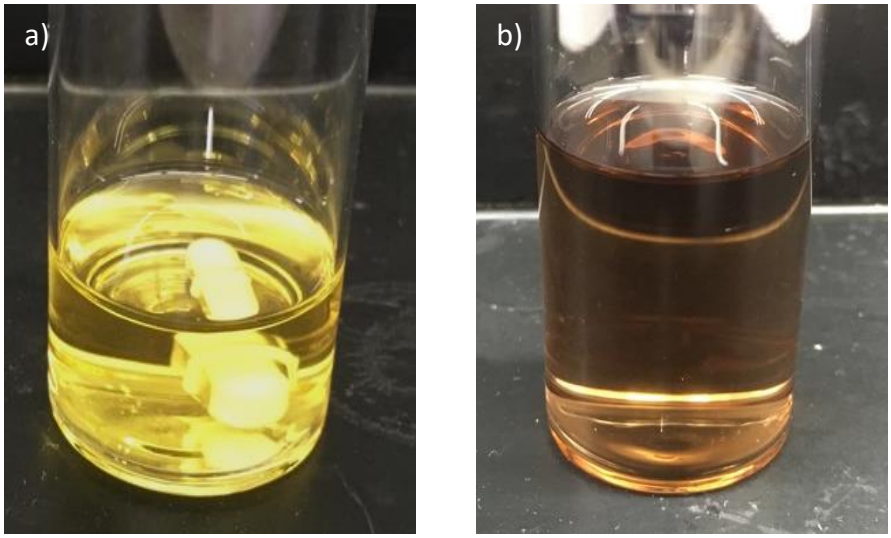

Fig. S7. Photographs of **3'-NP(D)** synthesis: a) **2(D)** in DCM before addition of $NaBH_4$ aqueous solution, b) **3'-NP(D)** after reaction being worked up and being re-dispersed in DCM.

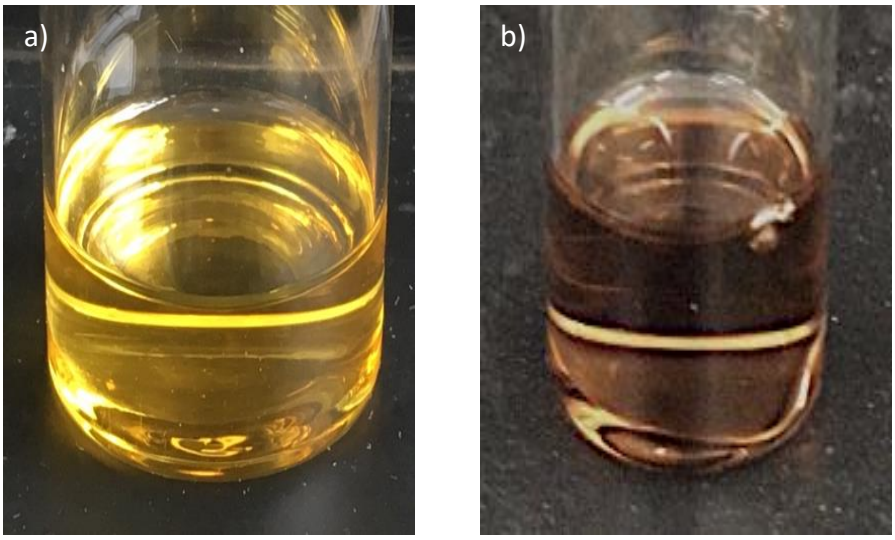

Fig. S8. UV-Vis absorption of **3'-NP(L)** in DCM

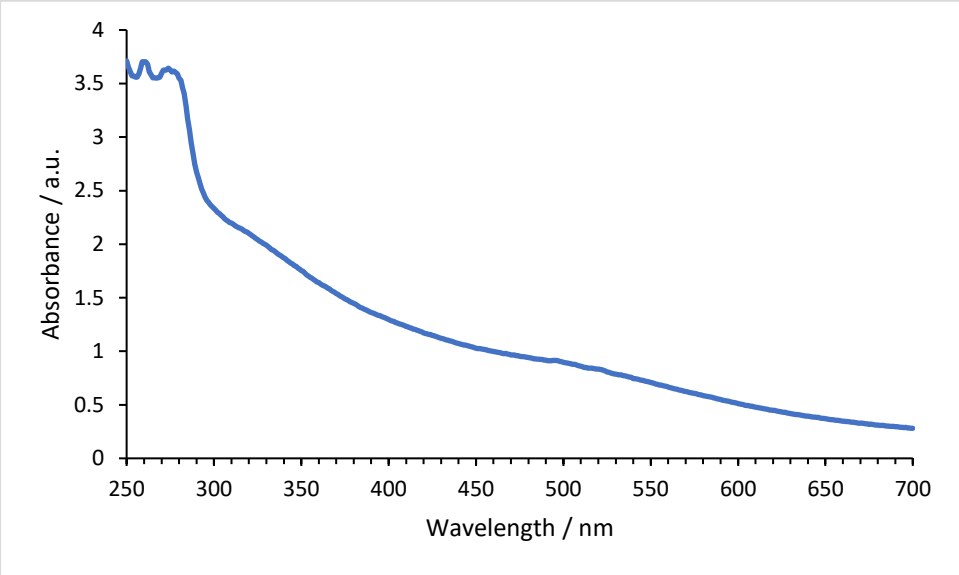

Zoomed in on 400-700 nm region.

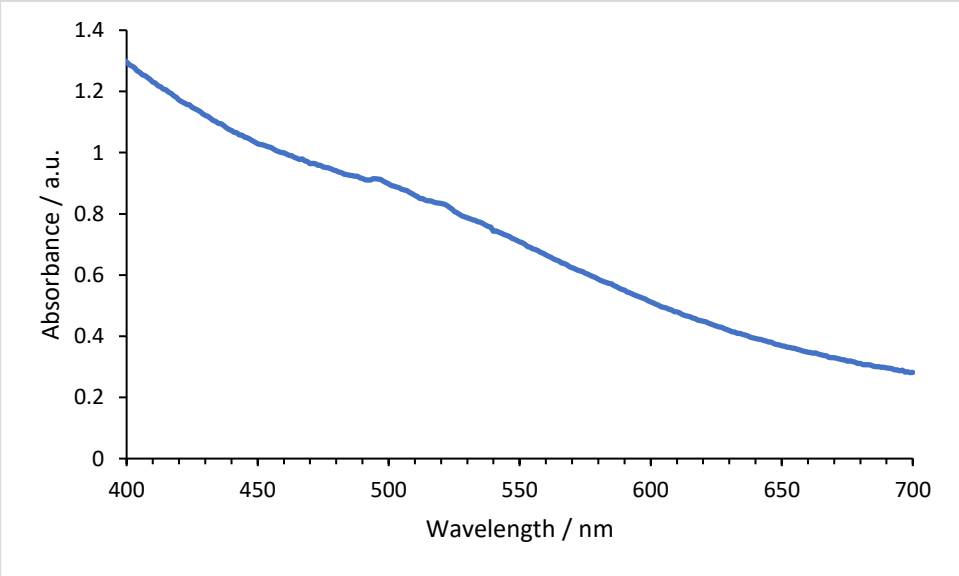

Fig. S9. UV-Vis absorption of **3'-NP(D)** in DCM

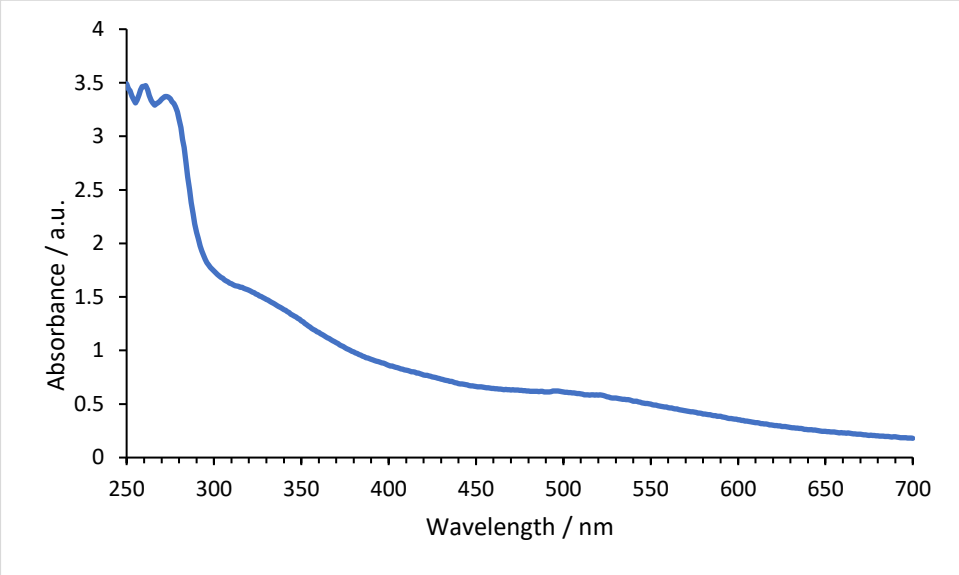

Zoomed in on 400-700 nm region.

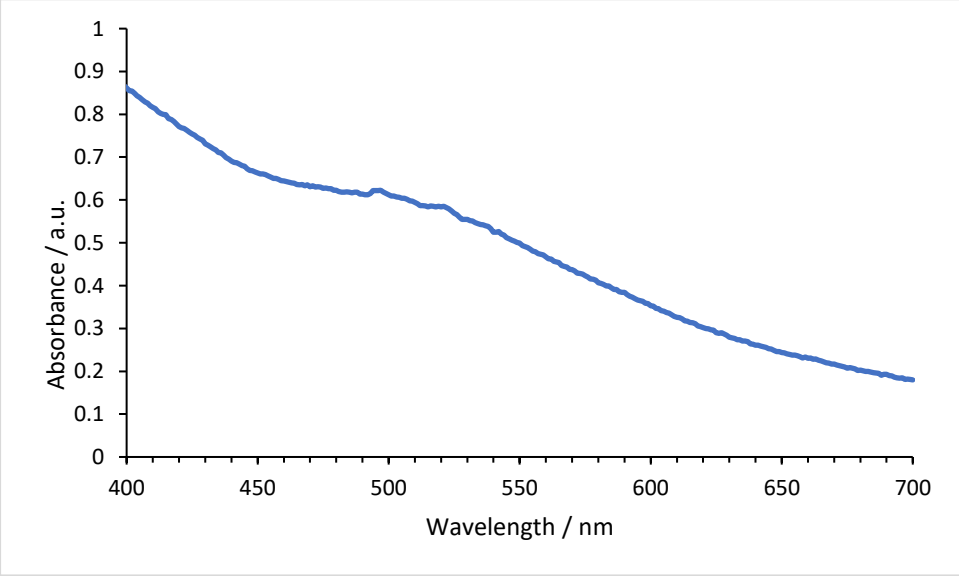

Fig. S10. UV-Vis absorption of **DDTAuNP** in toluene

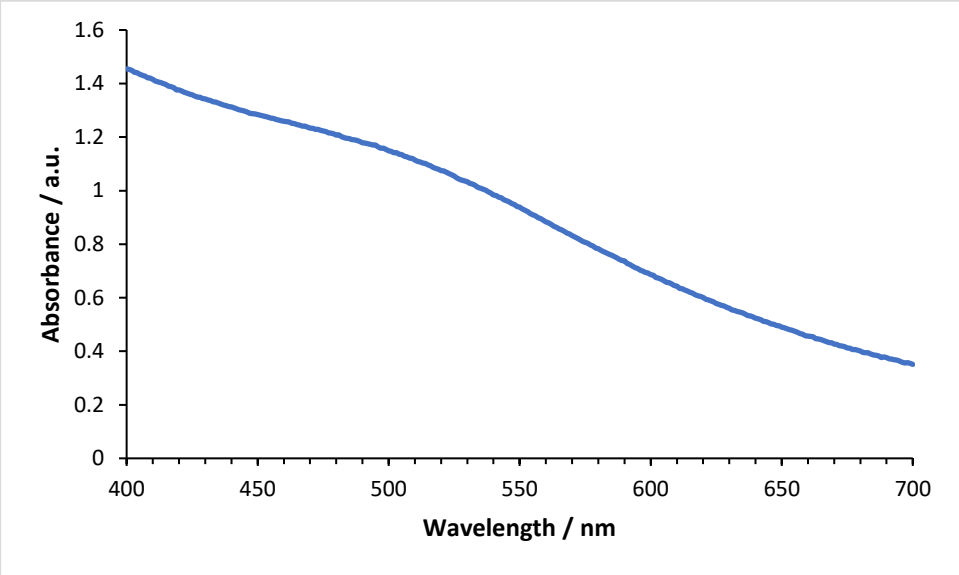

Fig. S11. DLS of **3'-NP(L)** in DCM

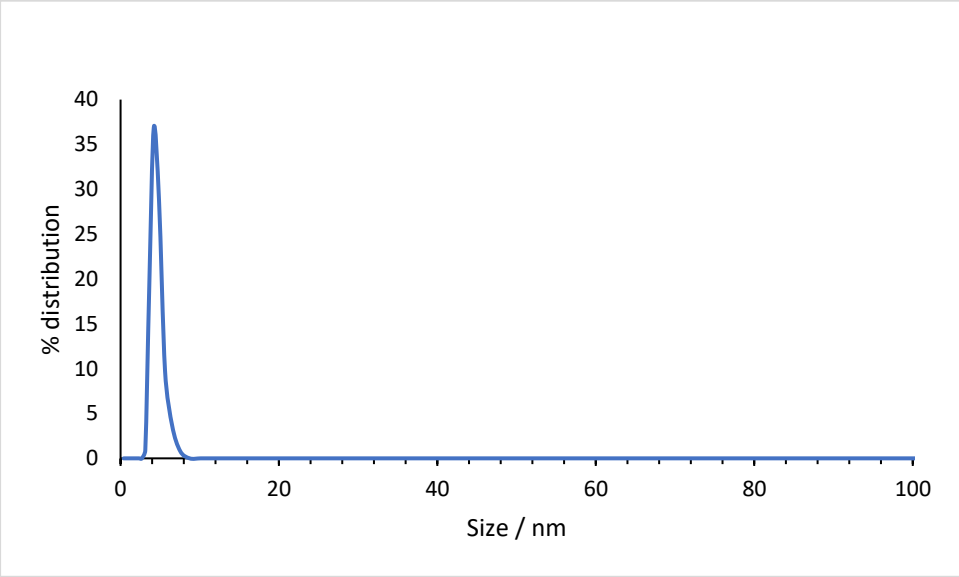

Size - 4.2 nm

Fig. S12. DLS of **3'-NP(D)** in DCM

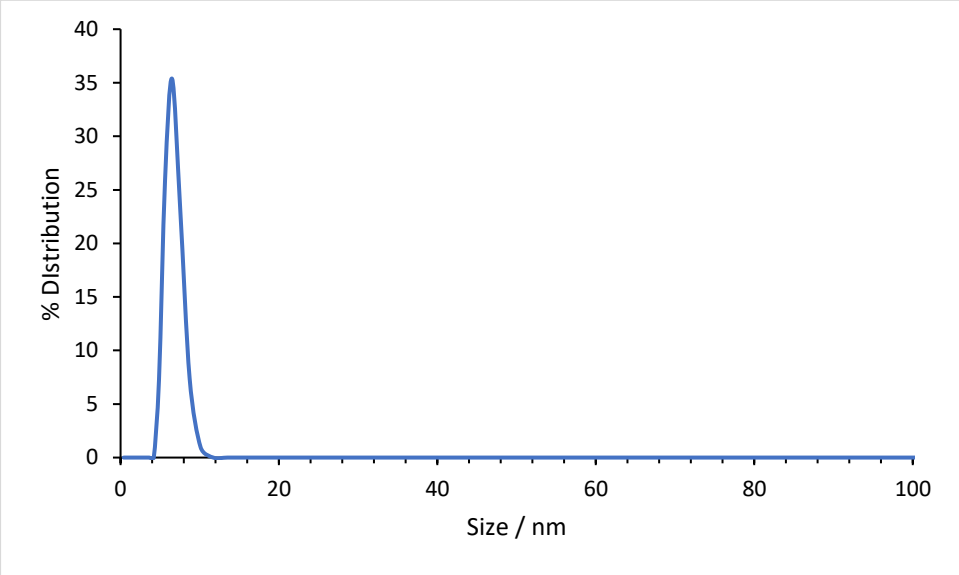

Size – 6.5 nm

Fig. S13. DLS of **DDTAuNP** in toluene

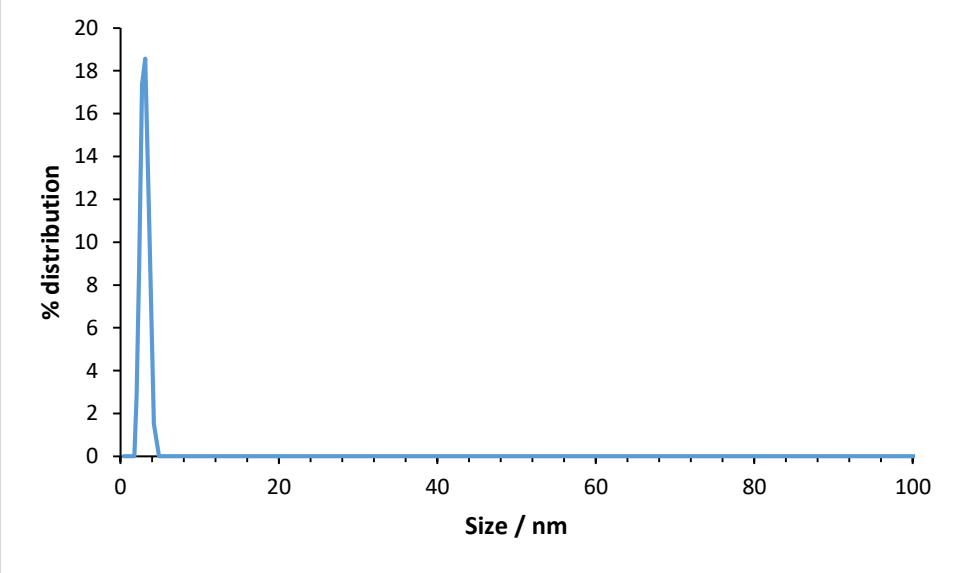

Size – 3.1 nm

Fig. S14. TGA of **2(L)**

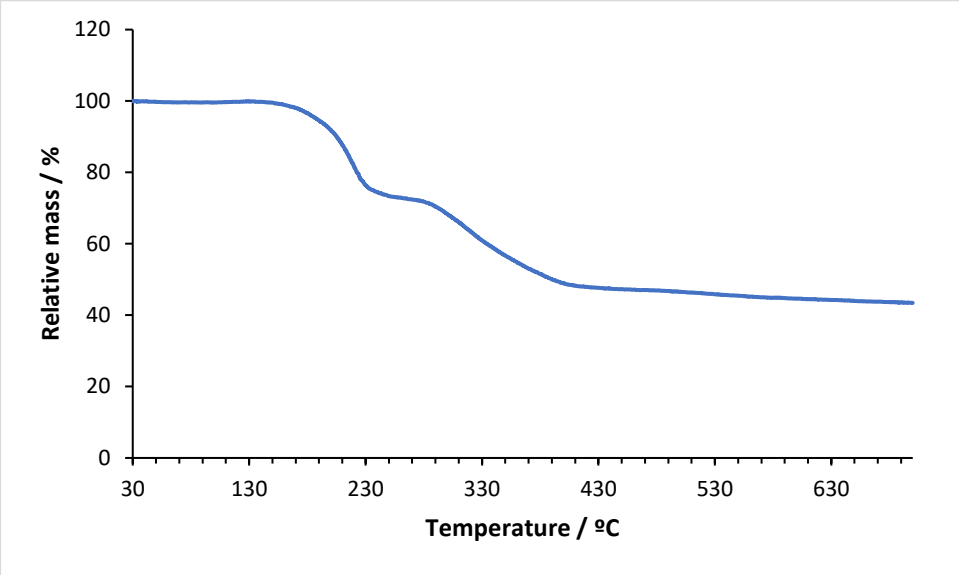

Organic component – 56.9%

Fig. S15. TGA of **2(D)**

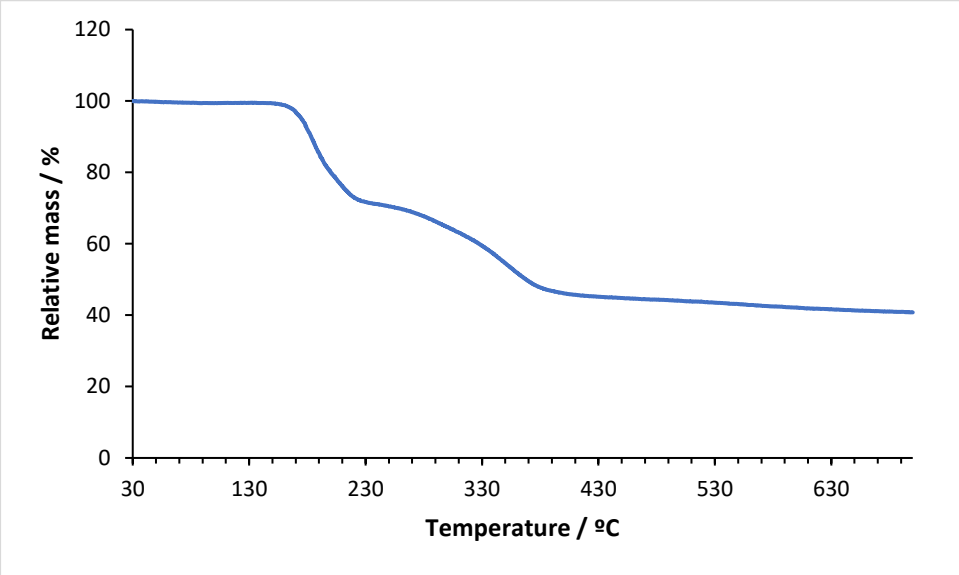

Organic component – 59.2%

Fig. S16. TGA of **3'-NP(L)**

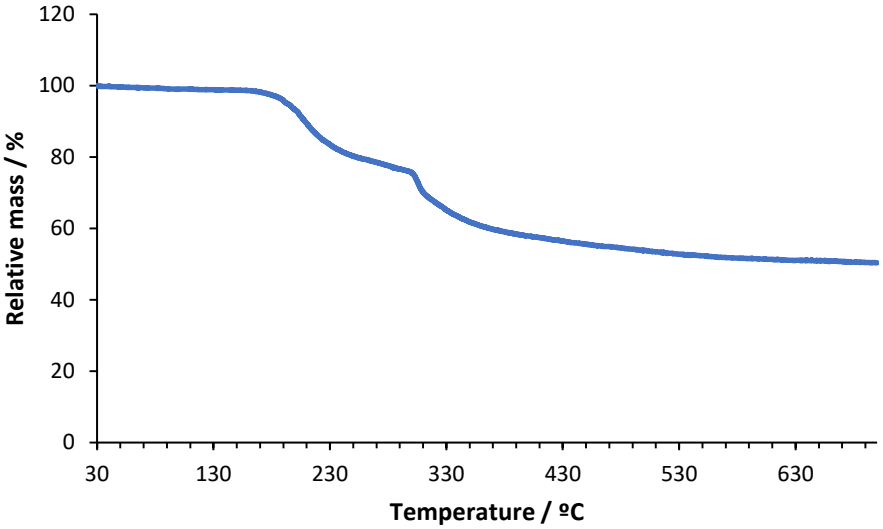

Organic component – 49.7 %

Fig. S17. TGA of **3'-NP(D)**

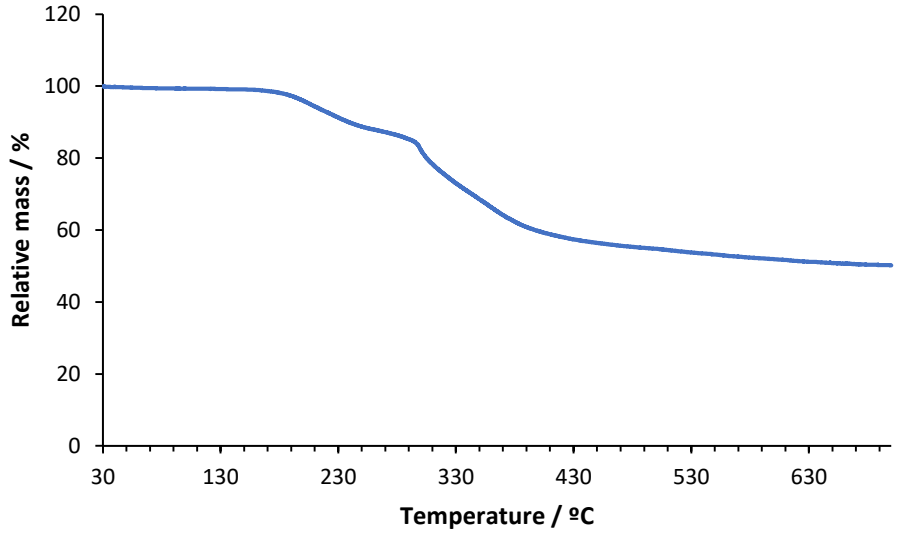

Organic component – 49.8 %

Fig. S18. TEM image of **3'-NP(L)**

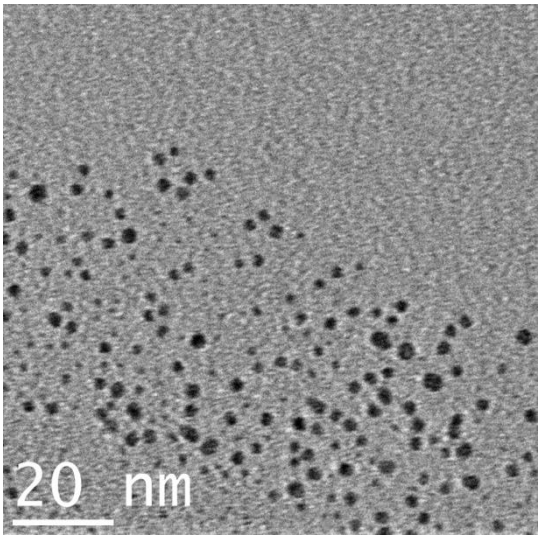

Fig. S19. TEM image of **3'-NP(D)**

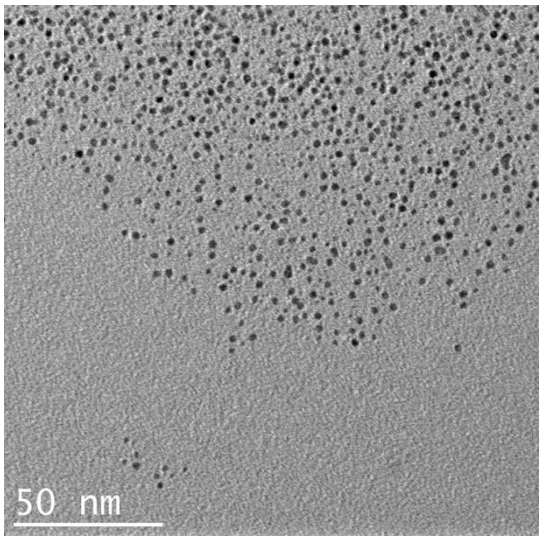

Fig. S20. TEM images of **DDTAuNP**

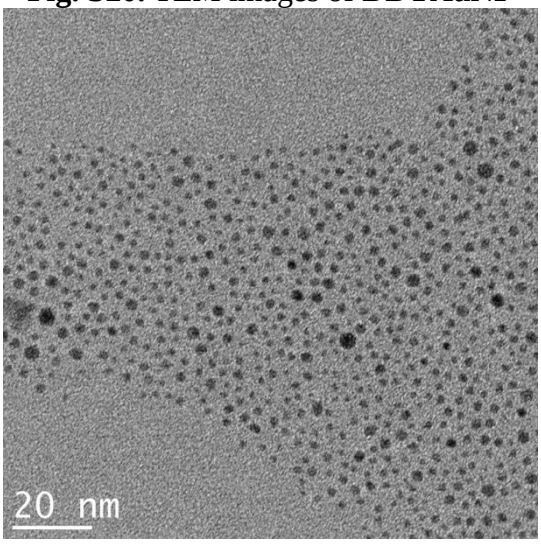

Fig. S21. UV-Vis spectra of **3'-NP(L)** in THF over a period of time

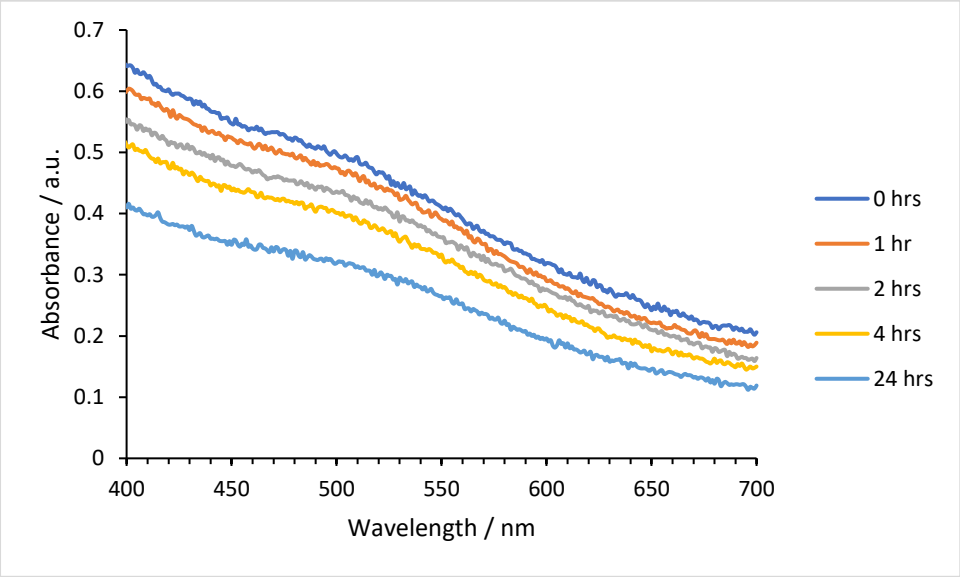

Fig. S22. UV-Vis spectra of **3'-NP(D)** in THF over a period of time

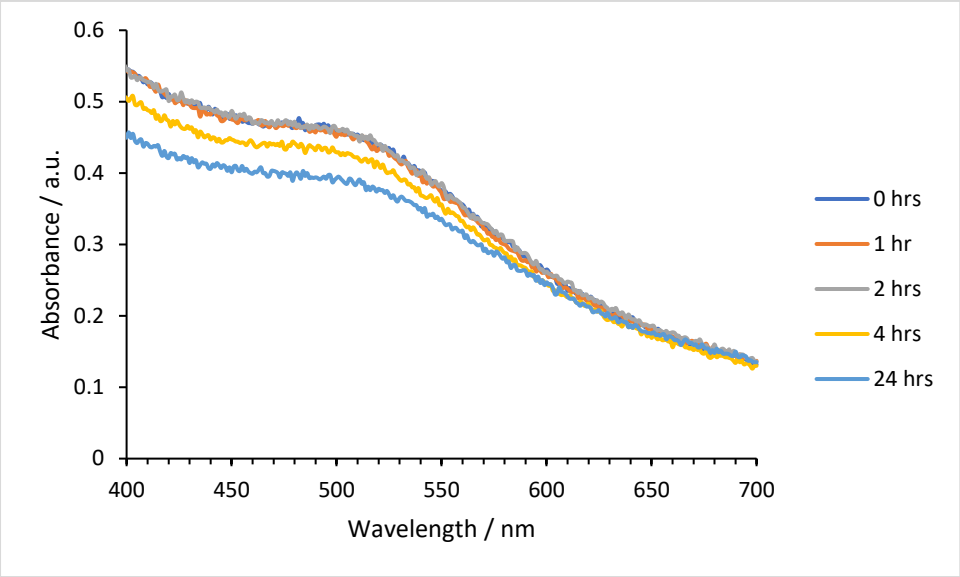

Fig. S23. UV-Vis spectra of **3'-NP(L)** refluxed in THF at 100 ºC over a time period

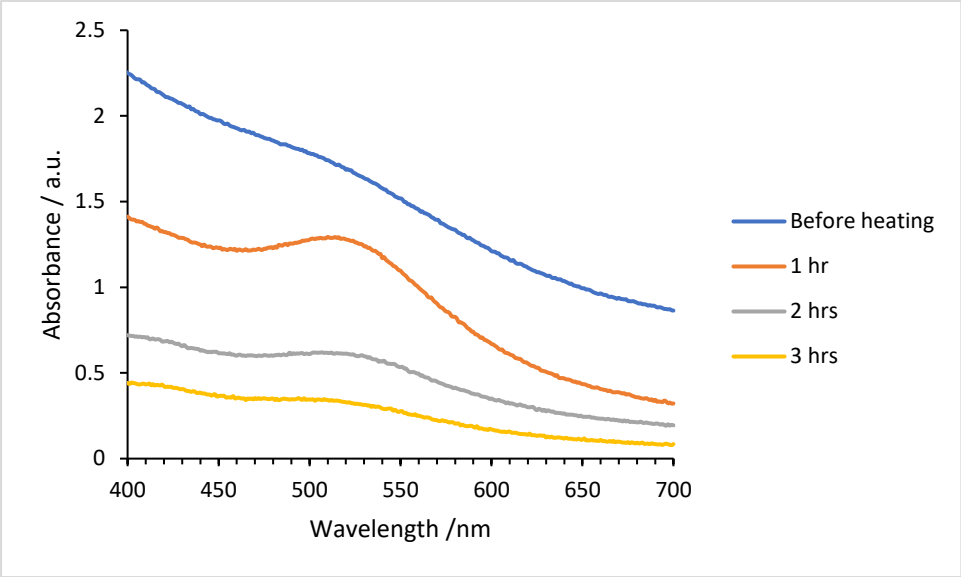

Fig. S24. UV-Vis spectra of **3'-NP(D)** refluxed in THF at 100 ºC over a time period

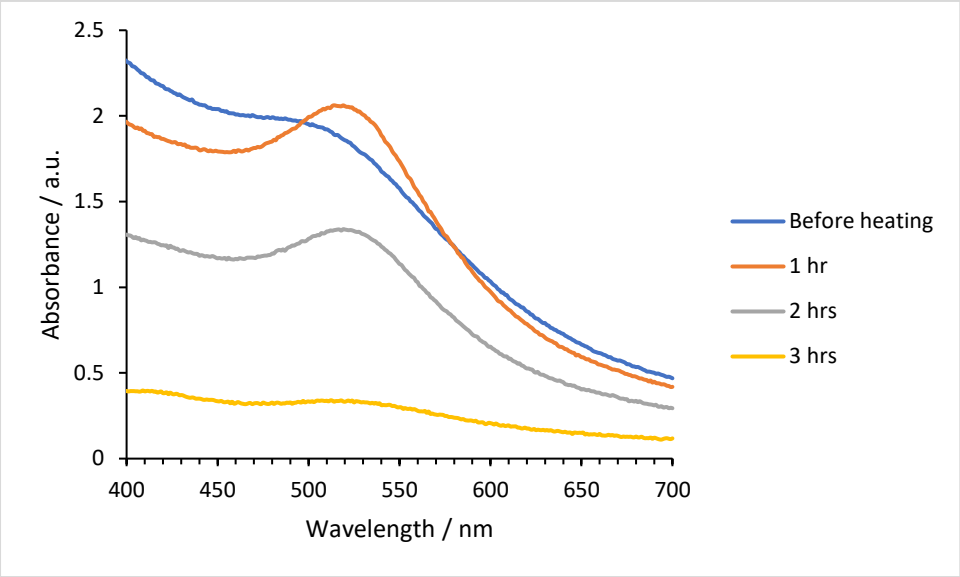

Fig. S25. UV-Vis spectra of **3'-NP(L)** refluxed in chloroform at 100 ºC over a time period

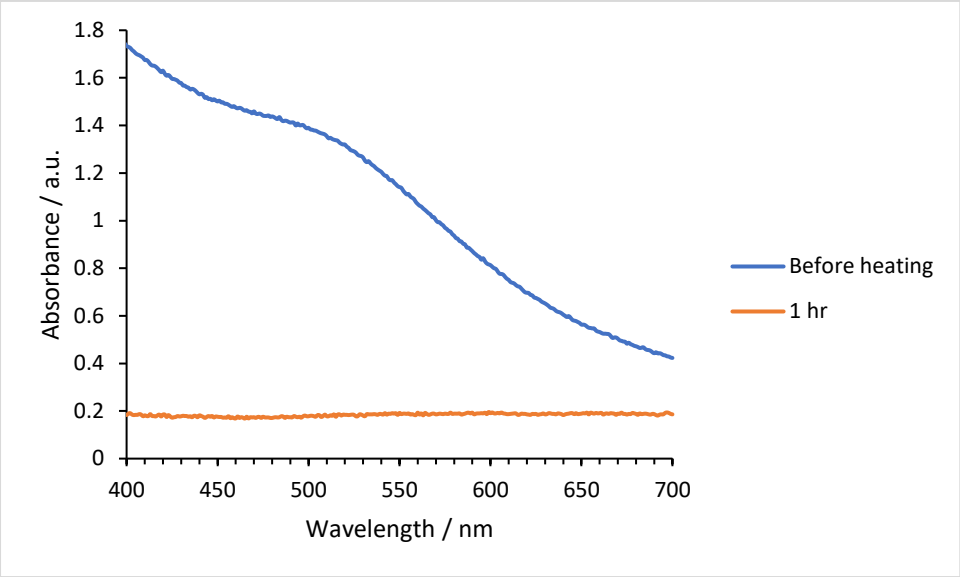

Fig. S26. UV-Vis spectra of **3'-NP(D)** refluxed in chloroform at 100 ºC over a time period

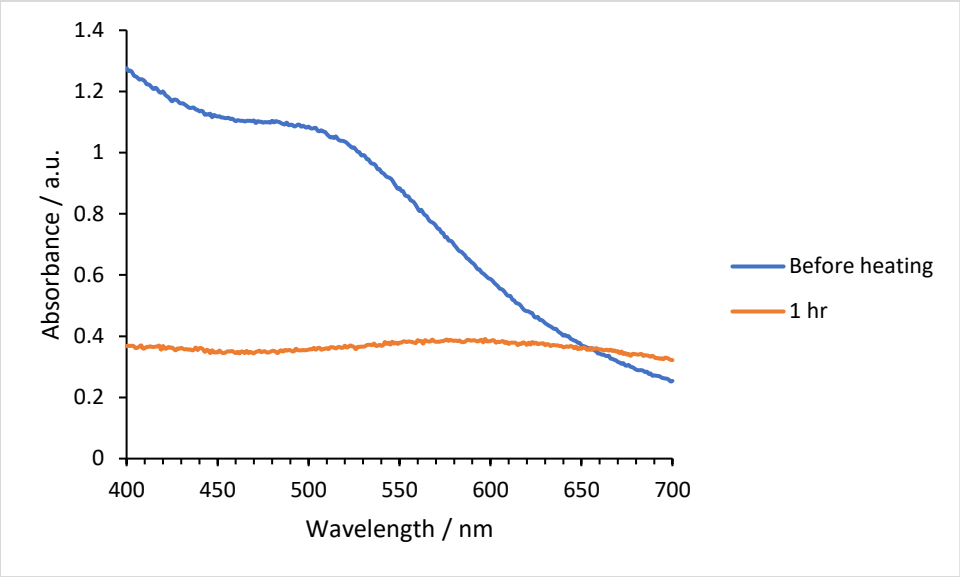

Fig. S27. UV-Vis spectra of **3'-NP(L)** heated in DMF at 100 ºC over a time period

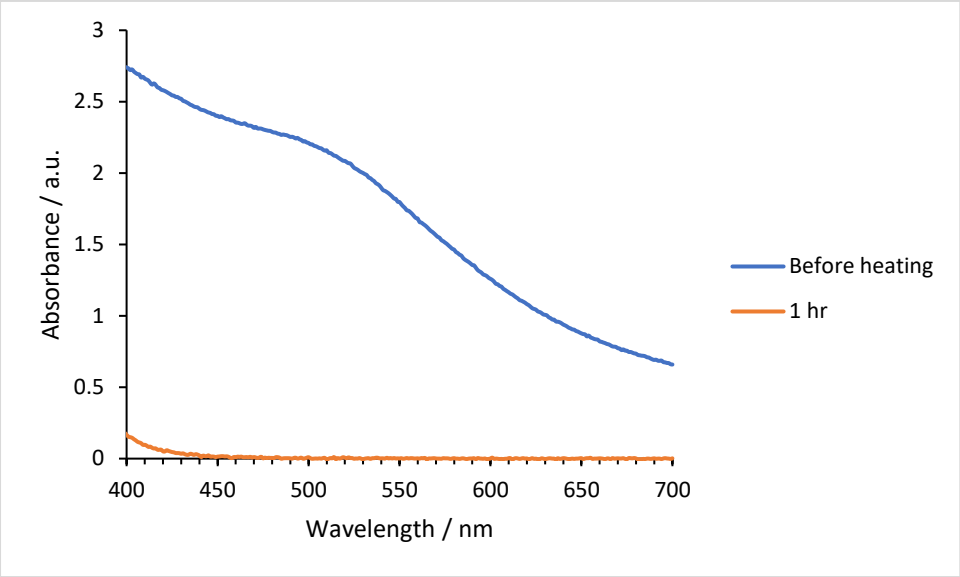

Fig. S28. UV-Vis spectra of **3'-NP(D)** heated in DMF at 100 ºC over a time period

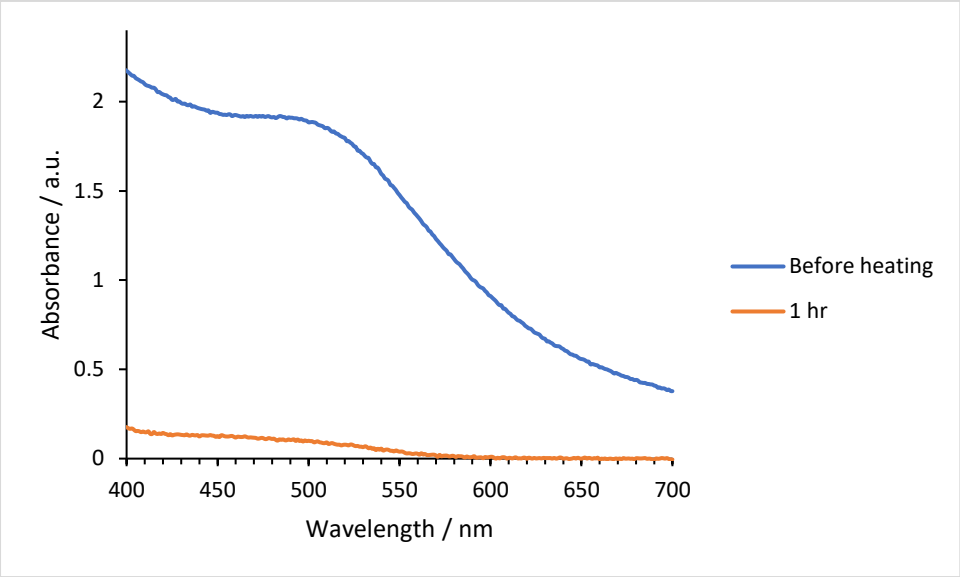

References

1. T. N. Hooper, C. P. Butts, M. Green, M. F. Haddow, J. E. McGrady and C. A. Russell, *Chemistry – A European Journal*, 2009, **15**, 12196-12200.
2. A. J. Young, C. J. Serpell, J. M. Chin and M. R. Reithofer, *Chem. Commun.*, 2017, **53**, 12426-12429.
3. S. Tougaard, *Surface and Interface Analysis*, 1997, **25**, 137-154.
4. D. A. Shirley, *Physical Review B*, 1972, **5**, 4709-4714.
5. J. H. Scofield, *J. Electron. Spectrosc. Relat. Phenom.*, 1976, **8**, 129-137.